nature ecology & evolution

ARTICLES

https://doi.org/10.1038/s41559-020-1243-1

Speleothem record attests to stable environmental conditions during Neanderthal–modern human turnover in southern Italy

Columbu Andrea[1]✉, Chiarini Veronica[1], Spötl Christoph[2], Benazzi Stefano[3,4], Hellstrom John[5], Cheng Hai[6,7,8] and De Waele Jo[1]

The causes of Neanderthal–modern human (MH) turnover are ambiguous. While potential biocultural interactions between the two groups are still little known, it is clear that Neanderthals in southern Europe disappeared about 42 thousand years ago (ka) after cohabitation for ~3,000 years with MH. Among a plethora of hypotheses on Neanderthal extinction, rapid climate changes during the Middle to Upper Palaeolithic transition (MUPT) are regarded as a primary factor. Here we show evidence for stable climatic and environmental conditions during the MUPT in a region (Apulia) where Neanderthals and MH coexisted. We base our findings on a rare glacial stalagmite deposited between ~106 and ~27 ka, providing the first continuous western Mediterranean speleothem palaeoclimate archive for this period. The uninterrupted growth of the stalagmite attests to the constant availability of rainfall and vegetated soils, while its $\delta^{13}C$–$\delta^{18}O$ palaeoclimate proxies demonstrate that Apulia was not affected by dramatic climate oscillations during the MUPT. Our results imply that, because climate did not play a key role in the disappearance of Neanderthals in this area, Neanderthal–MH turnover must be approached from a perspective that takes into account climatic and environmental conditions favourable for both species.

There is no leading theory about the triggers of the most important cultural transition in human history[1,2]. Rapid climate shifts during the Middle to Upper Palaeolithic transition (MUPT) are considered as one of the most important drivers of the Neanderthal–modern human (MH) interchange[2–8], because of the impact on population/depopulation dynamics[7,8], fragmentation of optimal habitats[6], deterioration of environmental conditions[3] and/or the weakening of local communities after severe cold and dry stages[4]. Accordingly, the Neanderthals were inexorably afflicted by recurrent millennial- to centennial-scale dry and cold conditions attributable to Dansgaard–Oeschger (DO) cycles and, in particular, Heinrich (H) events during marine isotope stage (MIS) 3. Heinrich events induced aridity and cold temperatures in Western and Central Europe[9], and those occurring from ~63–40.5 ka (H6–H4) had irreversible impacts on the Neanderthal population[5]. The H4 event caused the final demise and/or migration of Neanderthals to other areas, where extinction subsequently occurred[2]. However, this is at odds with the fact that H events lack consistent equivalents in the Mediterranean realm[10] and they may not necessarily have resulted in very harsh climatic conditions over the entire region[11]. Additionally, Neanderthal extinction might have occurred before H4 (ref. [12]). Indeed, there are chronological and spatial impediments in solving this conundrum because of age uncertainties for both palaeoclimatic and the anthropological events, and the unknown response of local Neanderthal–MH habitats to high-latitude-driven climatic change. Moreover, ancient human communities occupied only small portions of land with ideal settlement conditions, and the gradual climatic deterioration of the last glacial period probably reduced the extent of these optimal Neanderthal habitats[6]. Because the 2,600–5,400-year-long interval of Neanderthal–MH coexistence was probably unevenly distributed spatially[12], climate-related hypotheses should be based on records from the same area where Neanderthals–MH actually cohabitated, but these records are scarce[13].

Neanderthal and MH remains are widespread from northern to southern Italy[14]. This study targets Apulia (Fig. 1), where Neanderthals were present since at least MIS 5e until ~42 ka, while the earliest European MH appeared in this region ~45 ka (refs. [1,14]). This is therefore a strategic region in regard to understanding the biocultural processes occurring during the Neanderthal–MH transition and, ultimately, whether climate played a decisive role in the disappearance of the former and the territorial supremacy of the latter.

Results

We explored several caves in Apulia while searching for speleothems (Extended Data Fig. 1). Uranium–thorium (U–Th) radiometric dating on 14 stalagmites (Extended Data Fig. 5 and Supplementary Table 1) attests to the fact that cave calcite deposition was abundant during the last and older glacial periods (Fig. 1). Here we focus on stalagmite PC from Pozzo Cucù Cave (40.90° N, 17.16° E), from which 27 stratigraphically aligned U–Th dates (Supplementary Table 1) were used to produce an age–depth model (Extended Data Fig. 6). Accordingly, PC grew without interruption from $106.0^{+2.8}/_{-2.7}$ to $26.6^{+0.8}/_{-0.9}$ ka, and thus covers MIS 5–3 (Fig. 2). High-resolution $\delta^{18}O$–$\delta^{13}C$ analyses ($n = 2{,}659$) revealed a pattern comparable to

[1]Department of Biological, Geological and Environmental Sciences, University of Bologna, Bologna, Italy. [2]Institute of Geology, University of Innsbruck, Innsbruck, Austria. [3]Department of Cultural Heritage, University of Bologna, Bologna, Italy. [4]Department of Human Evolution, Max Planck Institute for Evolutionary Anthropology, Leipzig, Germany. [5]School of Earth Sciences, University of Melbourne, Melbourne, Victoria, Australia. [6]Institute of Global Environmental Change, Xi'an Jiaotong University, Xi'an, China. [7]State Key Laboratory of Loess and Quaternary Geology, Institute of Earth Environment, Chinese Academy of Sciences, Xi'an, China. [8]Department of Earth Sciences, University of Minnesota, Minneapolis, MN, USA. ✉e-mail: andrea.columbu2@unibo.it

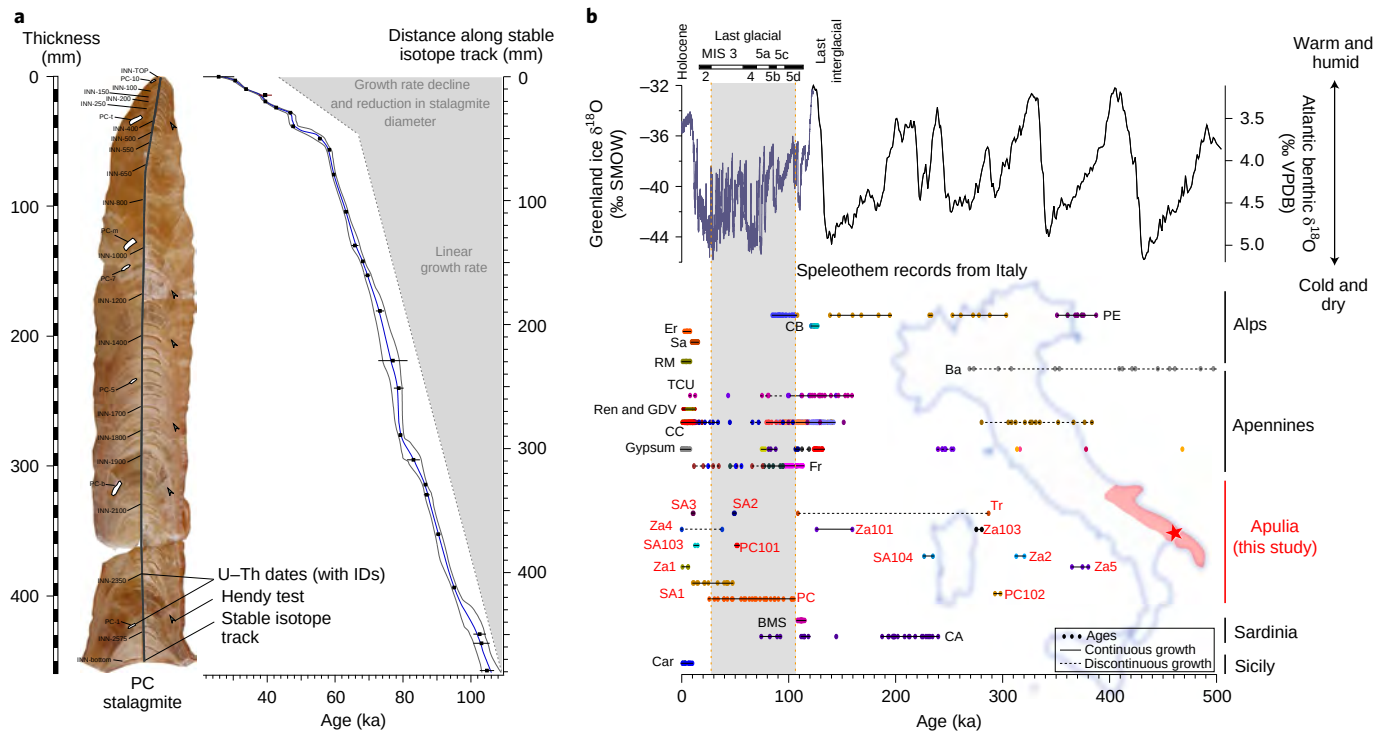

Fig. 1 | Cave samples. a, PC stalagmite, sampling information and age model (see Methods for age model construction and Hendy test). **b**, Ages of published Italian stalagmites used for palaeoclimate reconstruction and those presented in this study, compared to interglacial versus glacial variation over the past ~500ka (curves: Greenland ice core $\delta^{18}O$ (purple)[15] and benthic foraminifera $\delta^{18}O$ (black)[61]. The background shows a map of Italy with the location of the study caves (red star) and other published speleothem records. Ages are marked by dots, solid lines indicate continuous growth while dotted lines denote discontinuous growth and/or poor chronological constraint. Only speleothems from Apulia (this study, red labels) grew continuously over the entire last glacial period (grey shading). Speleothems: PE (Piani Eterni karst system)[48], Er (Ernesto Cave)[62], CB (Cesare Battisti Cave)[63], Sa (Savi Cave)[64], Ba (Basura Cave)[65], RM (Rio Martino Cave)[66], TCU (Tana che Urla Cave)[67], GDV (Grotta del Vento)[68], Ren (Renella Cave)[69], CC (Corchia Cave)[53], Gypsum (Northern Italy Gypsum caves)[70], Fr (Frasassi Cave)[16,54], SA (Sant'Angelo Cave, this study), Za (Zaccaria Cave, this study), Tr (Trullo Cave, this study), PC (Pozzo Cucù Cave, this study), BMS (Bue Marino Cave)[49], CA (Crovassa Azzurra Cave)[27], Car (Carburangeli Cave)[71]. SMOW, standard mean ocean water; VPDB, Vienna Pee Dee Belemnite.

the North Greenland Ice Core[15] (NGRIP) from the entire MIS 5 and 4. During MIS 3, $\delta^{18}O$ shows a less evident—but still recognizable—similarity to NGRIP while $\delta^{13}C$ yields a plateau-like signal. Importantly, $\delta^{18}O$–$\delta^{13}C$ does not show evidence of many of the most severe climatic events affecting northern latitudes (for example, H events).

Discussion

Because glacial stages in the Mediterranean area were generally dry and characterized by sparse vegetation, continuous speleothem growth was rare. In Italy, for example, there is no evidence of uninterrupted stalagmite deposition during glacial periods (Fig. 1). To our knowledge, the longest record was constructed using four speleothems (two stalagmites and two stalactites) found in Frasassi Cave[16]. In the Iberian Peninsula speleothem formation was also intermittent[10,17,18], while more continuous deposition is known only from caves in Turkey and on the south-eastern side of the Mediterranean Sea[19,20]. The continuous growth of speleothems in Manot Cave (Israel) has recently been taken as evidence for the absence of water shortage in northern Israel during the last glacial period[21]. Considering that continuous speleothem deposition is feasible only if the karst reservoir is recharged by rainfall and soil bioactivity accumulates high levels of CO_2 into infiltrating water, Apulia's glacial climate was possibly milder than in other areas in the western and central Mediterranean. The $\delta^{13}C$ values of PC are representative of soil activity[9,10] (see Methods). For most of that time, values are more negative than −5.0‰ (Fig. 2), attesting to the presence of C3 plants[22] that normally prevail in temperate regions.

It is well established that $\delta^{18}O$ in speleothems from the Mediterranean principally reflects variation in rainfall[23]. Secondarily, it might also record changes in moisture sources[24]. Because of the striking resemblance between PC-$\delta^{18}O$ and NGRIP $\delta^{18}O$ (Fig. 2), especially during MIS 5 and 4, we are confident that the stalagmite recorded the effects of climate change at high latitudes and in the North Atlantic. This intrahemispheric connection is translated into rainfall oscillations in Apulia during DO cycles, with higher (lower) rainfall during interstadials (stadials) as expressed by more negative (positive) $\delta^{18}O$ values in PC. This correlation can also be seen at the intra-interstadial time scale[25] (Extended Data Fig. 2). Intriguingly, the shape of several MIS 5 DO-like events in PC (for example, DOs from ~90 to ~70 ka) appears more similar to Asian monsoonal oscillations[26] than to NGRIP (Extended Data Fig. 3), a feature worth examining in detail in future studies. Variability in PC growth rate and $[^{234/238}U]_i$ (Extended Data Fig. 4) is in agreement with PC-$\delta^{18}O$ being driven principally by rainfall levels (see Methods). Changes in the dominant moisture source are possibly reflected also by PC-$\delta^{18}O$ values. During Greenland interstadials (GIs), rainfall in the Mediterranean region was predominantly Atlantic-sourced, giving rise to more negative $\delta^{18}O$ values similar to those currently recorded[23,27]. Conversely, Mediterranean-sourced moisture showing more positive $\delta^{18}O$ values prevailed when large ice sheets during Greenland stadials (GSs) impeded the westerlies

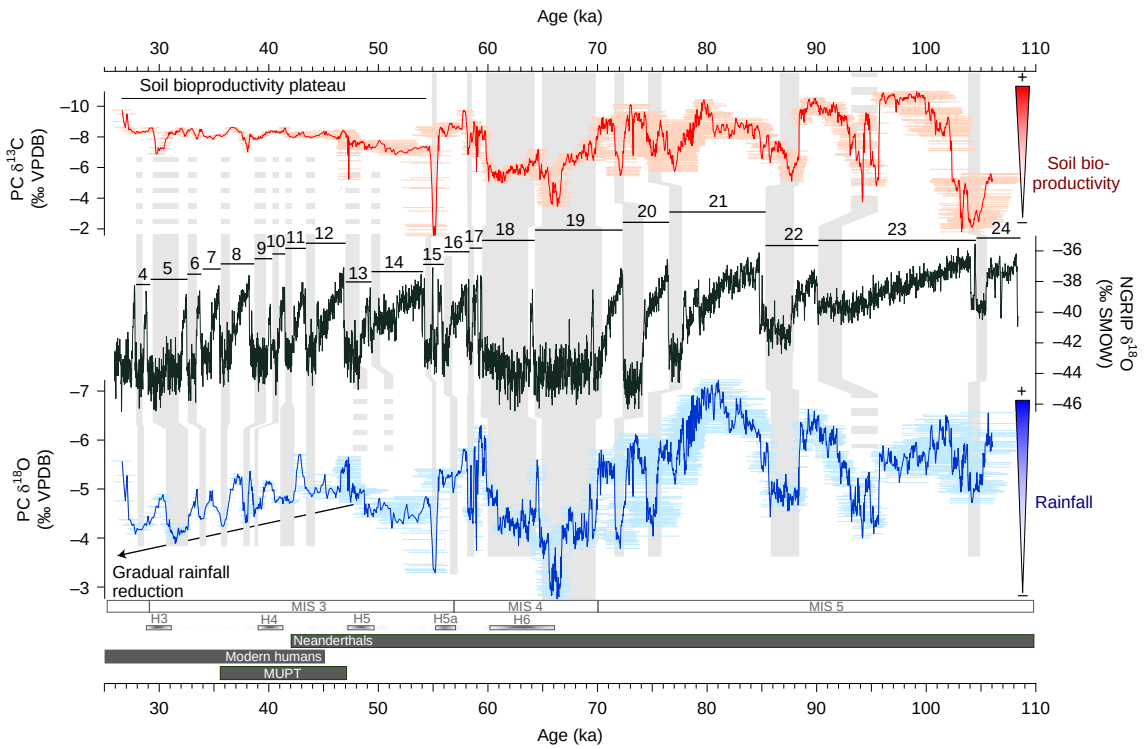

Fig. 2 | PC time series. PC $\delta^{13}C$ (top, red) and $\delta^{18}O$ (bottom, blue) versus Greenland ice core $\delta^{18}O$ (middle, black[15]). Black numbers and bars denote DO cycles[25]. The PC proxy record is correlated to NGRIP along stadial events (grey shading). Intermittent shading is used when correlation is ambiguous. Boxes at the bottom show MIS and H events, as well as the Neanderthal–MH transition in Apulia and MUPT in Europe. PC $\delta^{13}C$ and $\delta^{18}O$ curves also show age 2σ uncertainties (shaded horizontal bars).

from efficient delivery of moisture to the Mediterranean region (see Methods). This is because the lower moisture production in the Atlantic, according to the relative decrease in GS temperature, limits advection over the Mediterranean[23]. As Atlantic moisture input decreases, the ratio between Mediterranean/Atlantic moisture increases in the area of study. Further expansion of the northern ice sheet since MIS 3 probably resulted in a pronounced southward shift of the westerlies[24], which might have boosted this mechanism.

The covariation of $\delta^{18}O$ and $\delta^{13}C$ in PC is consistent with rainfall levels being a primary driver (Fig. 2). In Apulia, rainfall coupled with temperature variations, as recorded by other archives (Fig. 3), modulated soil organic activity reflected by the $\delta^{13}C$ record of PC (Fig. 2). Between DO 24 and 15, bioproductivity increased during GIs giving rise to more negative $\delta^{13}C$ values. Because of reduced rainfall and lower temperatures during GSs, bioproductivity decreased resulting in more positive $\delta^{13}C$ values. The generally low $\delta^{13}C$ values (that is, lower than ~5‰), in conjunction with an absence of growth pauses in PC, strongly argues for a continuously vegetated catchment of the cave's drip water, with expanding forests during GIs and trees becoming sparse during GSs (Fig. 3), in agreement with nearby pollen records[28,29]. The PC $\delta^{18}O$–$\delta^{13}C$ data suggest two periods of extremely dry conditions when both isotopes show peak values: from $66.7^{+0.9}/_{-1.2}$ to $65.6^{+1.1}/_{-1.3}$ ka during MIS 4, and from $55.3^{+1.1}/_{-2.5}$ to $54.9^{+1.1}/_{-2.7}$ ka during MIS 3. Both events deviate from NGRIP variability but are in agreement with speleothem[10], lacustrine[29] and marine records[30] from the Mediterranean region. They have been attributed to markedly dry conditions during ice-rafting events and increases in cold-water foraminifera in the North Atlantic during H events 6 and 5a[10,31]. Although the aridity of these events was not sufficient to stop carbonate deposition at the PC site, as occurred in speleothems from continental Europe[9] (Fig. 3g), these periods are regarded here as the driest and probably coldest of the entire MIS 5–3 time span, at least in southern Italy. The event at ~55 ka was certainly the driest of the entire record, as reflected by the highest $\delta^{13}C$ values and a marked reduction in growth rate (Fig. 1 and Extended Data Fig. 4). This event was probably even drier than GS24 and GS23, from $105.2^{+2.4}/_{-2.3}$ to $102.4^{+2.1}/_{-2.0}$ ka and from $95.7^{+0.9}/_{-0.8}$ to $93.1^{+0.7}/_{-0.9}$ ka, respectively, which also led to $\delta^{13}C$ values higher than −5‰.

There is no correlation between PC-$\delta^{18}O$ and NGRIP for DO 14 and 13 (Fig. 2), probably because of the low resolution resulting from the slow growth rate. From DO 12 to the top of the record, PC shows its most interesting features: (1) PC-$\delta^{18}O$ reveals NGRIP-like, millennial-scale oscillations although the similarities with NGRIP are strikingly less evident than before ~55 ka. The implication is that rapid climate oscillation during MIS 3 recorded in Greenland had a lower impact on rainfall variability in Apulia than during MIS 5 and 4; and (2) these oscillations are superimposed on a general PC-$\delta^{18}O$ trend toward more positive values (Fig. 2), which is synchronous with the progressive reduction in stalagmite diameter (Fig. 1). Considering that the latter mirrors long-lasting reduced dripping and thus calcite deposition at the top of the speleothem[32], these observations indicate a middle to upper MIS 3 in Apulia characterized by a progressive reduction in rainfall rather than by rapid and severe climate changes. At this point the Mediterranean might have become the primary source of moisture because of the expansion of the northern ice sheets. This is consistent with a gradual increase in the $\delta^{18}O$ value of the moisture source for PC. Furthermore, variation in rainfall during MIS 3 GIs and GSs, caused by Mediterranean cyclogenesis, is not comparable to that induced by a higher efficiency of westerlies delivering moisture during MIS 4 and 5. This is because the availability of moisture is lower than when the Atlantic is the principal moisture source. Most importantly, from ~55 ka onward PC $\delta^{13}C$ values show a plateau-like feature during MIS 3 (Fig. 2). This cannot be explained by in-karst processes and/or kinetic mechanisms affecting isotopic fractionation (see Methods),

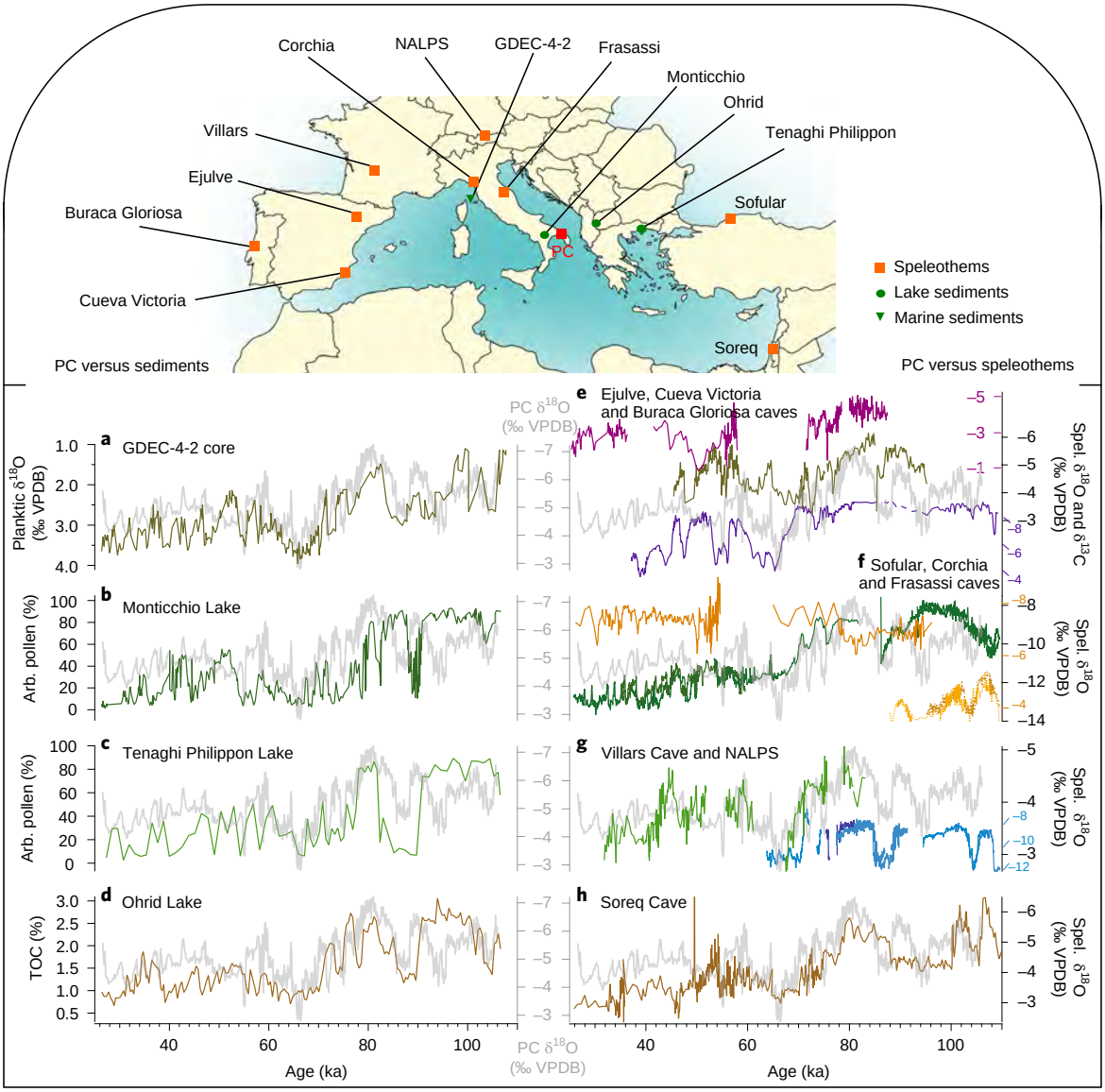

Fig. 3 | PC versus Mediterranean records. a–h, PC $\delta^{18}O$ record (grey) compared to marine (**a**, GDEC-4-2[30]) and lacustrine archives (**b**, Monticchio Lake[28]; **c**, Tenaghi Philippon Lake[29]; and **d**, Ohrid Lake[72]), as well as circum-Mediterranean speleothems (Spel.) (**e**, Cueva Victoria $\delta^{18}O$, yellow[17] (refer to *y*-axis/numbers), Ejulve Cave $\delta^{13}C$, purple[10], Buraca Gloriosa, pink[18]; **f**, Sofular Cave $\delta^{18}O$, green[19] (refer to *y*-axis/numbers), Corchia Cave $\delta^{18}O$, orange dotted line[53], Frasassi Cave (composite), orange[16]; **g**, Villars Cave $\delta^{18}O$, green[9], NALPS19 record $\delta^{18}O$, blue[73]; **h**, Soreq Cave $\delta^{18}O$, brown[20]). Arb., arboreal; TOC, total organic carbon.

but rather reflects stable soil dynamics and only minor vegetation changes. Preliminary $\delta^{18}O$–$\delta^{13}C$ data from another Apulian stalagmite (SA1; Fig. 2 and Extended Data Fig. 5) are in agreement with PC[33]. This reinforces the idea that drastic rainfall (and temperature) variations were minimal and insufficient to cause major changes in soil bioproductivity and/or interruptions in speleothem deposition. Speleothems from Frasassi Cave[16], the only Italian record available for comparison (Fig. 1), also report approximately constant $\delta^{18}O$–$\delta^{13}C$ (Fig. 3), from ~55 ka to at least ~30 ka, which was interpreted as mirroring relatively stable climatic conditions in the north-eastern Apennines. The slight depletion trend visible in the PC-$\delta^{13}C$ plateau may appear inconsistent with the gradual decrease in rainfall expressed by PC-$\delta^{18}O$. We advance the possibility that the absence of severe drought, which would also have caused total/partial soil erosion, allowed an enduring maturation of pedogenic layers despite the general trend of climatic deterioration. This hypothesis will be thoroughly explored in future studies. Vegetation shifts probably occurred, but these were possibly less pronounced than in the nearby Monticchio Lake[28] area (Fig. 3) because of the proximity to the coast and the lower altitude.

Accordingly, from ~55 ka onward, we set the beginning of environmental niche conditions in Apulia[1]. Neanderthals settled in this region well before MIS 3, so Apulia cannot be considered a refugium[34] for them. Contrary to the situation in Apulia, both freshwater availability and vegetation were scarce in the northern parts of the Italian peninsula, as highlighted by speleothem deposition (Fig. 1). This attracted wildlife and new hunter-gatherer communities in southern Italy.

Favourable settlement conditions may have fostered the arrival of MH in Apulia and their coexistence with Neanderthals (Fig. 2). The disappearance of Neanderthals in Apulia (~42 ka) occurred ~13,000 years after the cold and dry interval at ~55 ka, while the following H5 (~48 ka) apparently did not have a strong impact on the local environment. This is confirmed by arboreal pollen values

>40% in the nearby Monticchio Lake record[28]. In contrast, pollen in Greece[29], planktonic foraminifera in the Tyrrhenian Sea[30] and speleothems from Iberia[10] and Turkey[19] record climatic deterioration during H5 at ~48 ka (Fig. 3), further suggesting that Apulia was a favourable environmental niche during MIS 3 in comparison to other localities. It has recently been shown[35] that the climate in Morocco responded inconsistently to northern high-latitude, ice-rafted debris events, with even pluvial phases occurring during these cold and dry periods. This calls for a re-evaluation of the role of the northern high latitudes in triggering major cooling/drying events across the Mediterranean region. Even supposing a late Neanderthal presence in southern Italy—for example, later than ~42 ka—the fact that the impact of H4 (~40.5 ka) on PC proxy data is negligible further excludes climate as the major trigger for the Neanderthal–MH changeover during MUPT.

Final remarks

Because PC represents strong evidence of environmental stability in Apulia during the Neanderthal–MH turnover, rapid high-latitude climatic changes were not the primary cause of the disappearance of Neanderthals in this region. Opposite opinions face the paradox that shifts toward a dry and cold climate did not result in a cessation of speleothem deposition, but caused the extinction of a species well adapted to the surrounding environment and that survived previous climate periods more severe than MIS 3. Consequently, this applies to all European mid-latitude regions where DO climatic variations during MIS 3 were attenuated by latitudinal, orographic and/or geographical factors. In all niches similar to Apulia, the issue of Neanderthal–MH turnover must be approached from a perspective that takes into account climatic and environmental conditions favourable for both species. This, interestingly, differs from the situation in the Levantine area where there was no water shortage during MUPT, but speleothem $\delta^{13}C$ suggests an alternation between woody and more open vegetation. The adaptation of different modern cultures that possibly interacted with Neanderthals has been defined as landscape dependent in the Levantine area[21]. In niches similar to Apulia, instead, the advanced hunting technology of MH groups compared to that of Neanderthals since their migration to Europe[36–39] now appears a plausible explanation for the territorial supremacy of the former that induced the extinction of the latter after ~3,000 years of coexistence.

Methods

Cave sampling and speleothem subsampling. The caves explored for this work are Pozzo Cucù (40.90° N, 17.16° E), Trullo (40.85° N, 17.11° E), Sant'Angelo (40.73° N, 17.57° E) and Zaccaria (40.74° N, 17.55° E) (Extended Data Fig. 1). For conservation of the cave environment, all speleothems used in this study were found displaced from their original position, sometimes in multiple pieces. No hammers or any cutting tools were employed during sampling. PC stalagmite was found immediately adjacent to its growing location. All stalagmites were cut along the central axis and polished to allow better visualization of internal layering and macrofabrics. For U–Th ating, ~100 mg of calcite powders and/or chips was obtained by milling along a discrete number of growth layers. Drill bits of 1.0 and 0.8 mm were used for preliminary and detailed dating, respectively. For stable isotope subsampling, one-half of PC was quartered to perform precise milling along the central axis. The milling increments were 0.1 mm between the top and 51 mm from the top, and 0.2 from 51 mm to the bottom of the stalagmite. A total of 2,659 subsamples was obtained. See Fig. 1 for subsampling locations. The milling resulted in an average resolution of ~30 yr (range ~20–175 yr).

U–Th dating and $\delta^{13}C$–$\delta^{18}O$ analyses. The majority of U–Th dating was performed at the University of Melbourne (Australia), School of Earth Sciences, while a minor part was carried out at Xi'an Jiaotong University (China), Institute of Global Environmental Change (Supplementary Table 1). In Melbourne, ~100 mg of calcite was first dissolved using HNO_3 then spiked with a solution of known $^{236}U/^{233}U/^{229}Th$ ratio. Eichrom TRU-Spec resin columns were first decontaminated using a sequential wash of 1.5 M HNO_3, 4 M HCl and 0.2 M HF-0.1 M HCl, then the U + Th compound was separated from the carbonate matrix using another wash of 1.5 M HNO_3, 4 M HCl and 0.2 M HF-0.1 M HCl. The U + Th solution was evaporated on a hot plate at 80 °C and later mixed in 5% HNO_3-0.5% HF, and was then ready for analysis in a Nu Plasma multi-collector–inductively coupled plasma–mass spectrometer (MC–ICP–MS), with predefined settings[40]. Final U–Th ages were calculated using equation (1) of Hellstrom[41] using the ^{230}Th–^{234}U decay constants of Cheng et al.[42] and an initial $(^{230}Th/^{232}Th)_i$ of 1.5 ± 1.5.

In Xi'an the general chemical preparation procedure was similar to that in Melbourne except that U and Th compounds, after calcite HNO_3 dissolution, were first precipitated using a Fe solution then extracted separately using decontaminated resin columns and sequential washes of 6 N HCl and ultra-clean water. The U + Th solution was mixed with 2% HNO_3 + 0.1% HF before analysis on a Thermo Fisher Neptune Plus MC–ICP–MS[42]. Ages were calculated as above.

All ages are reported relative to 1950 bp (Supplementary Table 1). Despite slight differences in sample chemical treatment and age calculation, the dates produced in the two laboratories are consistent (Supplementary Table 1). Only the top and bottom were dated for the majority of speleothems (Extended Data Fig. 5), while 27 ages constitute the PC chronological dataset. The PC ages and their 2σ uncertainties were used in StalAge[43] and COPRA[44] to produce the age model. Both algorithms produced a comparable age–depth curve (Extended Data Fig. 6). To minimize intrinsic artefacts produced by the two algorithms, including unrealistic maxima in growth rate and unjustified large uncertainty propagation, the final age model was obtained by linear regression of average age values between StalAge and COPRA models at the same depths (Extended Data Fig. 6).

For stable isotopes, powders were prepared using an online, continuous-flow preparation system (GasBench II) then analysed with a Thermo Fisher Delta V Plus mass spectrometer at the University of Innsbruck (Austria), Institute of Geology. NBS18, NBS19, CO1 and CO8 standards were used as reference. The results are expressed in per-mill (‰) units relative to the Vienna Pee Dee Belemnite (VPDB) international standard. The 1σ analytical reproducibility was 0.06 and 0.08‰ for $\delta^{13}C$ and $\delta^{18}O$, respectively.

Conditions during PC deposition. Stable isotope values of speleothems deposited under non-equilibrium conditions may mask the palaeoclimate signal. The Hendy test can be used to evaluate geochemical conditions during calcite deposition[45], and equilibrium is indicated if: (1) $\delta^{13}C$ and $\delta^{18}O$ values are not strongly correlated along the growth axis; (2) $\delta^{13}C$ and $\delta^{18}O$ values are not strongly positively correlated from the centre to the flank along individual growth layers; and (3) $\delta^{13}C$ and $\delta^{18}O$ do not increase from the centre to the side of growth layer, with a maximum increase threshold of 0.8‰ for $\delta^{18}O$. $\delta^{13}C$ and $\delta^{18}O$ values along the central axis of PC are not strongly correlated ($r = 0.6$, although correlation itself might be a result of climate forcing[46]), and individual layers do not suggest non-equilibrium fractionation (Extended Data Fig. 7). A slight influence of kinetic fractionation is likely only for the H1 layer (Extended Data Fig. 7), located close to the top of the speleothem and starting at 10 mm from the centre of the stalagmite. In this top part, the stalagmite diameter is small and the more positive $\delta^{18}O$ values resulted from the steep flank.

In addition to the Hendy test, the constant ~10-cm diameter of PC also argues in favour of equilibrium-dominated isotope fractionation[47].

Finally, we consider Pozzo Cucù Cave a ventilation-poor environment during PC deposition, in view of the present narrow artificial entrance. Indeed, Pozzo Cucù possibly belongs to a karst system that had no large natural connection with the surface, minimizing air exchange between the cave and the surface. This is important because ventilation is the main driver of fast degassing and evaporation in caves (considering that humidity in non-ventilated caves is commonly close to condensation), with evaporation being one of the principal causes of kinetic fractionation. However, it is suspected that speleothems are never deposited under full equilibrium conditions[46] and we cannot exclude a small influence of kinetic fractionation in the PC stable isotope signature. For this reason, and based on our previous studies[27,48,49], PC is considered as having been deposited under quasi-equilibrium conditions—that is, $\delta^{13}C$ and $\delta^{18}O$ data primarily reflect palaeoclimate/palaeoenvironmental conditions above the cave.

Regarding post-depositional processes that might have compromised the original geochemical composition of the stalagmite, PC does not show any visual evidence of dissolution and recrystallization. Accordingly, all U–Th dates are in stratigraphic order (Supplementary Table 1).

Interpretation of $\delta^{13}C$ and $\delta^{18}O$ values. Speleothem $\delta^{13}C$ and $\delta^{18}O$ ($\delta^{13}C_{spel}$ and $\delta^{18}O_{spel}$) values reflect processes inside and outside of the karst system. Because endogenous (geological) processes might conceal and/or modify the geochemical output of exogenous (climatic) processes, the first challenge in speleothem science is to understand whether a potential climate signal has been registered in the stalagmite stable isotope signature. With calcite deposited under quasi-equilibrium conditions and with no evidence of diagenesis, endogenous factors can be ruled out as primary drivers of stable isotopic composition. Furthermore, considering that most PC $\delta^{13}C$ and $\delta^{18}O$ ($\delta^{13}C_{PC}$ and $\delta^{18}O_{PC}$) shifts occurred simultaneously with interhemispheric climatic events (Figs. 2 and 3), it is clear that climate played a major role in modulation of stable isotopes. The interpretation of $\delta^{13}C_{PC}$ and $\delta^{18}O_{PC}$ time series thus requires identification of the key exogenous factor(s), and understanding whether endogenous factors had a secondary role in modulation of $\delta^{13}C_{PC}$ and $\delta^{18}O_{PC}$ values.

At Western European latitudes, temperature and rainfall levels compete in the regulation of rainfall water $\delta^{18}O$ ($\delta^{18}O_{rw}$). Temperature and $\delta^{18}O_{rw}$ in the Mediterranean region show a weak positive gradient of ~0.22‰ °C^{-1}, while

rainfall amount and $\delta^{18}O_{rw}$ show a strong negative gradient of ~−1.6‰ 100 mm^{-1} rain[50]. The equilibrium $\delta^{18}O$ fractionation during calcite deposition ranges between −0.24‰ °C^{-1} (ref. [51]) and −0.18‰ °C^{-1} (ref. [52]), and counterbalances the temperature-dependent isotope fractionation of atmospheric precipitation outside the cave. Accordingly, rainfall amount is the principal driver of $\delta^{18}O_{spel}$ in the study area, as supported by previous studies in the western Mediterranean[18,23,27,48,49,53]. The same effect prevails in central Italy[54], the nearest speleothem record from Italy, as well as in Macedonia[55], the nearest speleothem record on the Balkan side of the Adriatic Sea. However, rainfall oscillations should also affect the rate of bedrock dissolution that, in turn, could have an important impact on growth rate and the abundance of uranium in speleothems. During wet (and warm) climate stages, bedrock is subjected to a more intense dissolution because of the higher quantity of water and a higher input of CO_2 from soil. Because of the higher amount of dissolved carbonate in drip water and potentially more rapid dripping in the cave, speleothem growth rate increases. The opposite (growth rate decrease) is expected for dry stages, although this general condition might not be valid for complex karst networks and/or might vary with time[56]. At the same time, rapid dissolution of bedrock limits uranium alpha-recoil and, ^{234}U and ^{238}U are leached equally from bedrock[23]. Longer water residence times, typical of drier conditions, promote uranium alpha-recoil and higher $[^{234/238}U]_i$ ratios because of a more efficient leaching of ^{234}U. If rainfall is the main regulator of $\delta^{18}O_{PC}$, more negative values are expected during relatively wet periods when growth rate increases and the $[^{234/238}U]_i$ ratio decreases; on the contrary, less negative values are expected during relatively dry periods when growth rate decreases and the $[^{234/238}U]_i$ ratio increases. PC shows, within uncertainties, this pattern, confirming that rainfall was one of the principal drivers of $\delta^{18}O_{PC}$ (Extended Data Fig. 4). Agreement between the $\delta^{18}O_{PC}$ pattern and the Greenland isotope record for most DO cycles, with more negative values during interstadials and less negative values during stadials, is an indirect confirmation of the rainfall effect because interstadials (stadials) were relatively wet (dry) in the Mediterranean realm[18,27,48,49,54].

Vegetation bioproductivity controls $\delta^{13}C$ of soil CO_2 ($\delta^{13}C_{soil}$) and thus $\delta^{13}C$ in infiltrating water ($\delta^{13}C_{iw}$). Excluding endogenous factors, $\delta^{13}C_{spel}$ ranges between −14.0 and −5.0‰ for C3 plants[22]. More negative $\delta^{13}C_{iw\text{-}spel}$ values are expected during periods of high bioproductivity, characteristic of humid and warm climate stages, while less negative $\delta^{13}C_{iw\text{-}spel}$ values are expected during periods of low bioproductivity, typical of dry and cold climate stages. $\delta^{13}C_{PC}$ shows the most evident oscillation during MIS 5 and 4, with lower values corresponding to interstadials and higher values corresponding to stadials, in agreement with $\delta^{18}O_{PC}$ oscillations. The only exogenous process that could cause a substantial increase in $\delta^{13}C_{iw\text{-}spel}$ is the switch to C4 vegetation[22]. At the same time, endogenous phenomena such as sulfide-driven bedrock dissolution[57], closed-system bedrock dissolution[45] and prior calcite precipitation (PCP)[58] also push $\delta^{13}C_{iw\text{-}spel}$ toward less negative values. Importantly, all of these processes can be attributed to a relatively dry climate, considering that C4 plants thrive in steppe-like environments and that endogenous processes are enhanced during times of reduced recharge. However, only PCP has an effect on both $\delta^{13}C_{iw\text{-}spel}$ and $\delta^{18}O_{iw\text{-}spel}$.

Concomitant variations in $\delta^{13}C_{PC}$ and $\delta^{18}O_{PC}$ during MIS 5–4 are thus attributed to rainfall amount and bioproductivity changes triggered by interstadial–stadial cyclicity. However, during the concomitant excursion toward the highest values at $105.2^{+2.4}/_{-2.3}$ ka, $95.7^{+0.9}/_{-0.8}$ to $93.1^{+0.7}/_{-0.9}$ ka, $66.7^{+0.9}/_{-1.2}$ to $65.6^{+1.1}/_{-1.3}$ ka and $55.3^{+1.1}/_{-2.5}$ to $54.9^{+1.1}/_{-2.7}$ ka and, especially when $\delta^{13}C_{PC}$ is above ~−5‰, it is possible that the above-mentioned processes may have played a role in increasing $\delta^{13}C_{PC}$ and $\delta^{18}O_{PC}$. We consider PCP as the main endogenous process increasing $\delta^{13}C_{iw}$ and $\delta^{18}O_{iw}$, because rapid shifts in $\delta^{13}C_{PC}$ and $\delta^{18}O_{PC}$ toward high values occur simultaneously. Sulfide-driven bedrock dissolution can be excluded because of the lack of sulfide minerals in the Pozzo Cucù bedrock.

During MIS 3, $\delta^{13}C_{PC}$ and $\delta^{18}O_{PC}$ do not covary. $\delta^{13}C_{PC}$ shows a pattern characterized by negligible oscillations with values around ~−8‰; $\delta^{18}O_{PC}$ shows millennial-scale DO-like oscillations of ~−1‰, lower than during MIS 5 and 4, and a general trend toward less negative values. The lack of covariation between $\delta^{13}C_{PC}$ and $\delta^{18}O_{PC}$ argues against PCP; mixing of groundwater or in-karst kinetic processes (for example, evaporation) is excluded for the same reason. The relatively negative values of ~−8‰ are inconsistent with closed-system and sulfide-driven bedrock dissolution. Even speleothems deposited from water in contact with CO_2 derived from old organic matter trapped in bedrock fissures would result in $\delta^{13}C$ values higher than ~−8‰. Thus $\delta^{13}C_{PC}$ reflects soil bioproductivity, which remained reasonably stable throughout MIS 3. This means that variations in rainfall amount (and temperature) during MIS 3 in Apulia were too small to cause perturbations in $\delta^{13}C_{soil}$. This limited rainfall variation, together with decreased resolution in this part of the record, could explain the small ~−1‰ excursions of $\delta^{18}O_{PC}$.

Finally, $\delta^{18}O_{PC}$ possibly responded to variations in moisture source during the entire MIS 5–3 period. Currently the study area receives most rainfall from the Atlantic, with a smaller contribution from the Mediterranean Sea[59]. Atlantic-sourced $\delta^{18}O_{rw}$ is more negative than Mediterranean-sourced $\delta^{18}O_{rw}$, and the influence of the former is related to (1) the abundance of moisture produced in the Atlantic and (2) the efficiency of westerlies delivering this moisture in the Mediterranean area. When polar ice sheets expanded, the influence of Atlantic-sourced moisture decreased in favour of Mediterranean-sourced moisture, because the production of moisture in the Atlantic is lower and the trajectories of the westerlies changed. With all other effects being negligible, the source effect[60] would generally follow DO cyclicity leading to more negative $\delta^{18}O$ values during interstadials and less negative values during stadials. However, at some point in MIS 3 the westerlies were pushed southward in response to expansion of the northern ice sheet. Rainfall in the Mediterranean was then controlled by the genesis of low-pressure areas (cyclones) within the Mediterranean realm. Although periods of increasing versus decreasing rainfall might still have followed regional-scale DO cyclicity, rainfall changes were less prominent than during MIS 5 and 4 because the availability of moisture is lower than when the Atlantic is the principal moisture source. A possible interpretation of the $\delta^{18}O_{PC}$ signature during MIS 3 invokes a major influence of Mediterranean-derived rainfall causing a gradual trend of rainfall reduction, with a superimposed low-intensity rainfall increase versus decrease pattern (following DO cyclicity). It is important to stress that both the gradual reduction and decrease in rainfall during MIS 3 GIs in Apulia were insufficient to cause perturbations in $\delta^{13}C_{soil}$ as, for example, during MIS 5 and 4.

Reporting Summary. Further information on research design is available in the Nature Research Reporting Summary linked to this article.

Data availability

Data supporting this study are available in Supplementary Table 1 and Supplementary Table 2.

Received: 5 February 2020; Accepted: 9 June 2020;
Published online: 06 July 2020

References

1. Benazzi, S. et al. Early dispersal of modern humans in Europe and implications for Neanderthal behaviour. *Nature* **479**, 525–529 (2011).
2. Wolf, D. et al. Climate deteriorations and Neanderthal demise in interior Iberia. *Sci. Rep.* **8**, 7048 (2018).
3. Mellars, P. A new radiocarbon revolution and the dispersal of modern humans in Eurasia. *Nature* **439**, 931–935 (2006).
4. Müller, U. C. et al. The role of climate in the spread of modern humans into Europe. *Quat. Sci. Rev.* **30**, 273–279 (2011).
5. Staubwasser, M. et al. Impact of climate change on the transition of Neanderthals to modern humans in Europe. *Proc. Natl Acad. Sci. USA* **115**, 9116–9121 (2018).
6. Melchionna, M. et al. Fragmentation of Neanderthals' pre-extinction distribution by climate change. *Palaeogeogr. Palaeoclimatol. Palaeoecol.* **496**, 146–154 (2018).
7. Finlayson, C. & Carrion, J. S. Rapid ecological turnover and its impact on Neanderthal and other human populations. *Trends Ecol. Evol.* **22**, 213–222 (2007).
8. Stewart, J. R. The ecology and adaptation of Neanderthals during the non-analogue environment of Oxygen Isotope Stage 3. *Quat. Int.* **137**, 35–46 (2005).
9. Genty, D. et al. Precise dating of Dansgaard–Oeschger climate oscillations in western Europe from stalagmite data. *Nature* **42**, 833–837 (2003).
10. Pérez-Mejías, C. et al. Orbital-to-millennial scale climate variability during Marine Isotope Stages 5 to 3 in northeast Iberia. *Quat. Sci. Rev.* **224**, 105946 (2019).
11. Badino, F. et al. An overview of Alpine and Mediterranean palaeogeography, terrestrial ecosystems and climate history during MIS 3 with focus on the Middle to Upper Palaeolithic transition. *Quat. Int.* https://doi.org/10.1016/j.quaint.2019.09.024 (2019).
12. Higham, T. et al. The timing and spatiotemporal patterning of Neanderthal disappearance. *Nature* **512**, 306–309 (2014).
13. Rey-Rodríguez, I. et al. Last Neanderthals and fi st anatomically modern humans in the NW Iberian Peninsula: climatic and environmental conditions inferred from the Cova Eirós small-vertebrate assemblage during MIS 3. *Quat. Sci. Rev.* **151**, 185–197 (2016).
14. Benazzi, S. et al. The makers of the Protoaurignacian and implications for Neandertal extinction. *Science* **348**, 793–796 (2015).
15. NGRIP Members. High-resolution record of Northern Hemisphere climate extending into the last interglacial period. *Nature* **431**, 147–151 (2004).
16. Kudielka, G. et al. in *250 Million Years of Earth History in Central Italy: Celebrating 25 Years of the Geological Observatory of Coldigioco* Vol. 542 (eds Koeberl, C. & Bice, D. M.) 429–445 (Geological Society of America, 2019); https://doi.org/10.1130/2019.2542(24).
17. Budsky, A. et al. Western Mediterranean climate response to Dansgaard/Oeschger events: new insights from speleothem secords. *Geophys. Res. Lett.* **46**, 9042–9053 (2019).
18. Denniston, R. F. et al. A stalagmite test of North Atlantic SST and Iberian hydroclimate linkages over the last two glacial cycles. *Clim. Past* **14**, 1893–1913 (2018).

19. Badertscher, S. et al. Pleistocene water intrusions from the Mediterranean and Caspian seas into the Black Sea. *Nature Geosci.* **4**, 236–239 (2011).
20. Bar-Matthews, M., Ayalon, A., Gilmour, M., Matthews, A. & Hawkesworth, C. J. Sea–land oxygen isotopic relationships from planktonic foraminifera and speleothems in the Eastern Mediterranean region and their implication for paleorainfall during interglacial intervals. *Geochim. Cosmochim. Acta* **67**, 3181–3199 (2003).
21. Yasur, G. et al. Climatic and environmental conditions in the Western Galilee, during Late Middle and Upper Paleolithic periods, based on speleothems from Manot Cave, Israel. *J. Hum. Evol.* https://doi.org/10.1016/j.jhevol.2019.04.004 (2019).
22. McDermott, F. Palaeo-climate reconstruction from stable isotope variations in speleothems: a review. *Quat. Sci. Rev.* **23**, 901–918 (2004).
23. Drysdale, R. N. et al. Evidence for obliquity forcing of glacial Termination II. *Science* **325**, 1527–1531 (2009).
24. Luetscher, M. et al. North Atlantic storm track changes during the Last Glacial Maximum recorded by Alpine speleothems. *Nat. Commun.* **6**, 6344 (2015).
25. Rasmussen, S. O. et al. A stratigraphic framework for abrupt climatic changes during the Last Glacial period based on three synchronized Greenland ice-core records: refini g and extending the INTIMATE event stratigraphy. *Quat. Sci. Rev.* **106**, 14–28 (2014).
26. Cheng, H. et al. The climatic cyclicity in semiarid-arid central Asia over the past 500,000 years. *Geophys. Res. Lett.* **39**, L01705 (2012).
27. Columbu, A. et al. A long record of MIS 7 and MIS 5 climate and environment from a western Mediterranean speleothem (SW Sardinia, Italy). *Quat. Sci. Rev.* **220**, 230–243 (2019).
28. Allen, J. R. M. et al. Rapid environmental changes in southern Europe during the last glacial period. *Science* **400**, 740–743 (1999).
29. Tzedakis, P. C., Hooghiemstra, H. & Pälike, H. The last 1.35 million years at Tenaghi Philippon: revised chronostratigraphy and long-term vegetation trends. *Quat. Sci. Rev.* **25**, 3416–3430 (2006).
30. Toucanne, S. et al. Tracking rainfall in the northern Mediterranean borderlands during sapropel deposition. *Quat. Sci. Rev.* **129**, 178–195 (2015).
31. Hodell, D. A., Channell, J. E. T., Curtis, J. H., Romero, O. E. & Röhl, U. Onset of "Hudson strait" Heinrich events in the eastern North Atlantic at the end of the middle Pleistocene transition (~640 ka)?: Pleistocene Heinrich events. *Paleoceanography* **23**, PA4218 (2008).
32. Kaufmann, G. & Dreybrodt, W. Stalagmite growth and palaeo-climate: an inverse approach. *Earth Planet. Sci. Lett.* **224**, 529–545 (2004).
33. Columbu, A. et al. A long continuous palaeoclimate-palaeoenvironmental record of the last glacial period from southern Italy and implications for the coexistence of Anatomically Modern Humans and Neanderthals. *Proc. European Geosciences Union (EGU) Conference* https://doi.org/10.5194/egusphere-egu2020-140 (2020).
34. Stewart, J. & Stringer, B. Human evolution out of Africa: the role of refugia and climate change. *Science* **335**, 1317–1321 (2012).
35. Ait Brahim, Y. et al. North Atlantic ice-rafting, ocean and atmospheric circulation during the Holocene: insights from Western Mediterranean speleothems. *Geophys. Res. Lett.* **46**, 7614–7623 (2019).
36. Sano, K. et al. The earliest evidence for mechanically delivered projectile weapons in Europe. *Nat. Ecol. Evol.* **3**, 1409–1414 (2019).
37. Arrighi, S. et al. Backdating systematic shell ornament making in Europe to 45,000 years ago. *Archaeol. Anthropol. Sci.* **12**, 59 (2020).
38. Arrighi, S. et al. Bone tools, ornaments and other unusual objects during the Middle to Upper Palaeolithic transition in Italy. *Quat. Int.* https://doi.org/10.1016/j.quaint.2019.11.016 (2019).
39. Marciani, G. et al. Lithic techno-complexes in Italy from 50 to 39 thousand years BP: an overview of lithic technological changes across the Middle–Upper Palaeolithic boundary. *Quat. Int.* https://doi.org/10.1016/j.quaint.2019.11.005 (2019).
40. Drysdale, R. N. et al. Precise microsampling of poorly laminated speleothems for U-series dating. *Quat. Geochronol.* **14**, 38–47 (2012).
41. Hellstrom, J. U–Th dating of speleothems with high initial 230Th using stratigraphical constraint. *Quat. Geochronol.* **1**, 289–295 (2006).
42. Cheng, H. et al. Improvements in ^{230}Th dating, ^{230}Th and ^{234}U half-life values, and U–Th isotopic measurements by multi-collector inductively coupled plasma mass spectrometry. *Earth Planet. Sci. Lett.* **371–372**, 82–91 (2013).
43. Scholz, D. & Hoffmann, D. L. StalAge – an algorithm designed for construction of speleothem age models. *Quat. Geochronol.* **6**, 369–382 (2011).
44. Breitenbach, S. F. M. et al. COnstructing Proxy-Record Age models (COPRA). *Clim. Past* **8**, 1765–1779 (2012).
45. Hendy, C. H. The isotopic geochemistry of speleothems-I. The calculation of the effects of different modes of formation on the isotopic composition of speleothems and their applicability as palaeoclimatic indicators. *Geochim. Cosmochim. Acta* **35**, 801–824 (1971).
46. Mickler, P. J., Stern, L. A. & Banner, J. L. Large kinetic isotope effects in modern speleothems. *Geol. Soc. Am. Bull.* **118**, 65–81 (2006).
47. Dreybrodt, W. & Scholz, D. Climatic dependence of stable carbon and oxygen isotope signals recorded in speleothems: from soil water to speleothem calcite. *Geochim. Cosmochim. Acta* **75**, 734–752 (2011).
48. Columbu, A., Sauro, F., Lundberg, J., Drysdale, R. & De Waele, J. Palaeoenvironmental changes recorded by speleothems of the southern Alps (Piani Eterni, Belluno, Italy) during four interglacial to glacial climate transitions. *Quat. Sci. Rev.* **197**, 319–335 (2018).
49. Columbu, A. et al. Early last glacial intra-interstadial climate variability recorded in a Sardinian speleothem. *Quat. Sci. Rev.* **169**, 391–397 (2017).
50. Bard, E. et al. Hydrological conditions over the western Mediterranean basin during the deposition of the cold Sapropel 6 (ca. 175 kyr BP). *Earth Planet. Sci. Lett.* **202**, 481–494 (2002).
51. Kim, S.-T. & O'Neil, J. R. Equilibrium and nonequilibrium oxygen isotope effects in synthetic carbonates. *Geochim. Cosmochim. Acta* **61**, 3461–3475 (1997).
52. Tremaine, D. M., Froelich, P. N. & Wang, Y. Speleothem calcite farmed in situ: modern calibration of δ^{18}O and δ^{13}C paleoclimate proxies in a continuously-monitored natural cave system. *Geochim. Cosmochim. Acta* **75**, 4929–4950 (2011).
53. Drysdale, R. N. et al. Stalagmite evidence for the precise timing of North Atlantic cold events during the early last glacial. *Geology* **35**, 77–80 (2007).
54. Vanghi, V. et al. Climate variability on the Adriatic seaboard during the last glacial inception and MIS 5c from Frasassi Cave stalagmite record. *Quat. Sci. Rev.* **201**, 349–361 (2018).
55. Regattieri, E. et al. A MIS 9/MIS 8 speleothem record of hydrological variability from Macedonia (F.Y.R.O.M.). *Glob. Planet. Change* **162**, 39–52 (2018).
56. Ford, D. & Williams, P. *Karst Geomorphology and Hydrology* (John Wiley & Sons, 2007).
57. Bajo, P. et al. Stalagmite carbon isotopes and dead carbon proportion (DCP) in a near-closed-system situation: an interplay between sulphuric and carbonic acid dissolution. *Geochim. Cosmochim. Acta* **210**, 208–227 (2017).
58. Fairchild, I. J. & Treble, P. C. Trace elements in speleothems as recorders of environmental change. *Quat. Sci. Rev.* **28**, 449–468 (2009).
59. Longinelli, A. & Selmo, E. Isotopic composition of precipitation in Italy: a fi st overall map. *J. Hydrol.* **270**, 75–88 (2003).
60. Dansgaard, W. Stable isotopes in precipitation. *Tellus* **16**, 436–468 (1964).
61. Lisiecki, L. E. & Raymo, M. E. A Pliocene–Pleistocene stack of 57 globally distributed benthic δ^{18}O records. *Paleoceanography* **20**, PA1003 (2005).
62. Frisia, S., Borsato, A., Preto, N. & McDermott, F. Late Holocene annual growth in three Alpine stalagmites records the influence of solar activity and the North Atlantic Oscillation on winter climate. *Earth Planet. Sci. Lett.* **216**, 411–424 (2003).
63. Johnston, V. E. et al. Evidence of thermophilisation and elevation-dependent warming during the Last Interglacial in the Italian Alps. *Sci. Rep.* **8**, 2680 (2018).
64. Belli, R. et al. Regional climate variability and ecosystem responses to the last deglaciation in the northern hemisphere from stable isotope data and calcite fabrics in two northern Adriatic stalagmites. *Quat. Sci. Rev.* **72**, 146–158 (2013).
65. Pozzi, J. P. et al. U–Th dated speleothem recorded geomagnetic excursions in the Lower Brunhes. *Sci. Rep.* **9**, 1114 (2019).
66. Regattieri, E. et al. Holocene Critical Zone dynamics in an Alpine catchment inferred from a speleothem multiproxy record: disentangling climate and human influences. *Sci. Rep.* **9**, 17829 (2019).
67. Regattieri, E. et al. A continuous stable isotope record from the penultimate glacial maximum to the Last Interglacial (159–121 ka) from Tana Che Urla Cave (Apuan Alps, central Italy). *Quat. Res.* **82**, 450–461 (2014).
68. Isola, I. et al. Speleothem U/Th age constraints for the Last Glacial conditions in the Apuan Alps, northwestern Italy. *Palaeogeogr. Palaeoclimatol. Palaeoecol.* **518**, 62–71 (2019).
69. Zhornyak, L.V. et al. Stratigraphic evidence for a "pluvial phase" between ca 8200–7100 ka from Renella cave (Central Italy). *Quat. Sci. Rev.* **30**, 409–417 (2011).
70. Columbu, A. et al. Late quaternary speleogenesis and landscape evolution in the northern Apennine evaporite areas. *Earth Surf. Process. Landf.* **42**, 1447–1459 (2017).
71. Frisia, S. et al. Holocene climate variability in Sicily from a discontinuous stalagmite record and the Mesolithic to Neolithic transition. *Quat. Res.* **66**, 388–400 (2006).
72. Francke, A. et al. Sedimentological processes and environmental variability at Lake Ohrid (Macedonia, Albania) between 637 ka and the present. *Biogeosciences* **13**, 1179–1196 (2016).
73. Moseley, G. E. et al. NALPS19: sub-orbital scale climate variability recorded in Northern Alpine speleothems during the last glacial period. *Clim. Past* **16**, 29–50 (2020).

Acknowledgements

We thank all local speleologists that helped with the 2014 and 2019 fieldwork at Pozzo Cucù, Sant'Angelo, Zaccaria and Messapi caves: G. Loperfido, S. Inguscio, G. Ragone, P. Lippolis, A. Lacirignola, D. Leserri, M. Marraffa, O. Lacarbonara, F. Semeraro, S. Calella, P. Calella, C. Pastore, C. Marchitelli, R. Romanazzi, R. Cupertino, G. Caló and F. Lorusso (Gruppo Speleologico Martinese, CARS Altamura, Gruppo Speleologico Neretino, Gruppo Ricerche Carsiche Putignano, Gruppo Puglia Grotte and Gruppo Escursionistico Speleologico Ostunense), as well as the Bellanova family for access to Messapi Cave. C.A., D.W.J. and C.V. are also grateful to all members of Gruppo Speleologico Martinese for their logistic help and warm hospitality in Martina Franca. Thanks also to M. Parise (University of Bari) for help during 2014 fieldwork; A. Reina (Polytechnic University of Bari) for his enthusiasm in supporting this research; V. Casulli and R. Laragione of Castellana Grotte for their interest in supporting this study; M. Wimmer and M. Luetscher (Innsbruck University) for their help during laboratory work; L. Pisani (Bologna University) for the DEM figure used in Extended Data Fig. 1; and L. Calabrò (Bologna University) for drilling of sample SA1. C.A. is supported by Leonardo Da Vinci Grant 2019 (DD MIUR, no. 787, 15/04/2019); B.S. is supported by ERC grant no. 724046—SUCCESS (https://ERC-SUCCESS.eu), and C.H. by NSFC grant no. 41888101. This research received financial contributions from both Grotte di Castellana and Federazione Speleologica Pugliese.

Author contributions

C.A. and C.V. conceived and designed the experiments. C.A., C.V., S.C., H.J. and C.H. performed the experiments. C.A. and B.S. analysed the data. C.A., C.V., S.C., B.S. and D.W.J. contributed with materials and analysis tools. C.A. wrote the paper with input from all co-authors.

Competing interests

The authors declare no competing interests

Additional information

Extended data is available for this paper at https://doi.org/10.1038/s41559-020-1243-1.

Supplementary information is available for this paper at https://doi.org/10.1038/s41559-020-1243-1.

Correspondence and requests for materials should be addressed to C.A.

Reprints and permissions information is available at www.nature.com/reprints.

Publisher's note Springer Nature remains neutral with regard to jurisdictional claims in published maps and institutional affiliations.

© The Author(s), under exclusive licence to Springer Nature Limited 2020

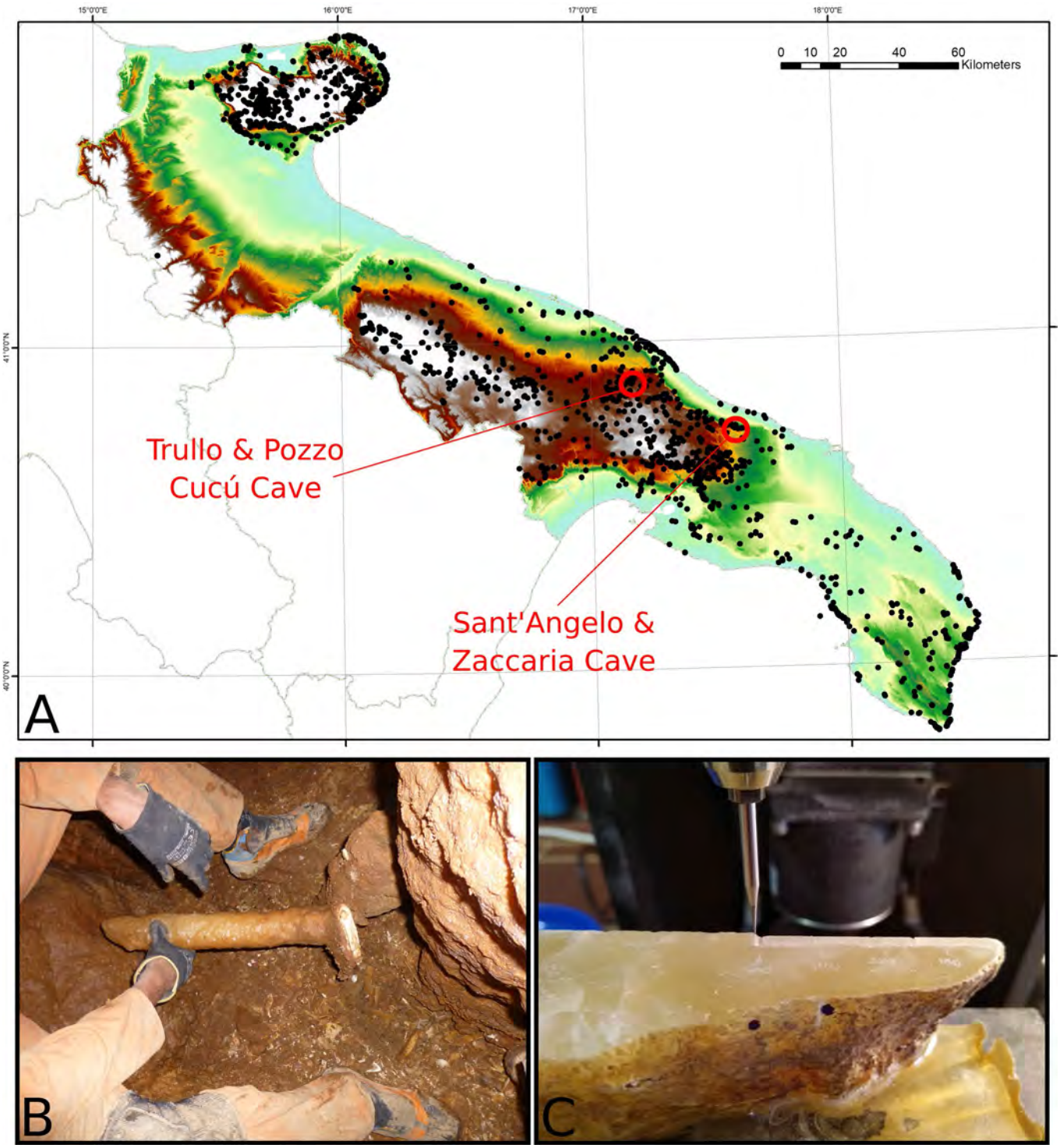

Extended Data Fig. 1 | Cave locations and sampling. a) Apulia region with colour-coded topography; black dots indicate major caves in Puglia (from http://www.catasto.fspuglia.it/), while red circles report caves explored for this project. **b**) PC stalagmite found close to its original growth position. **c**) PC milling subsampling for $\delta^{18}O$ and $\delta^{13}C$.

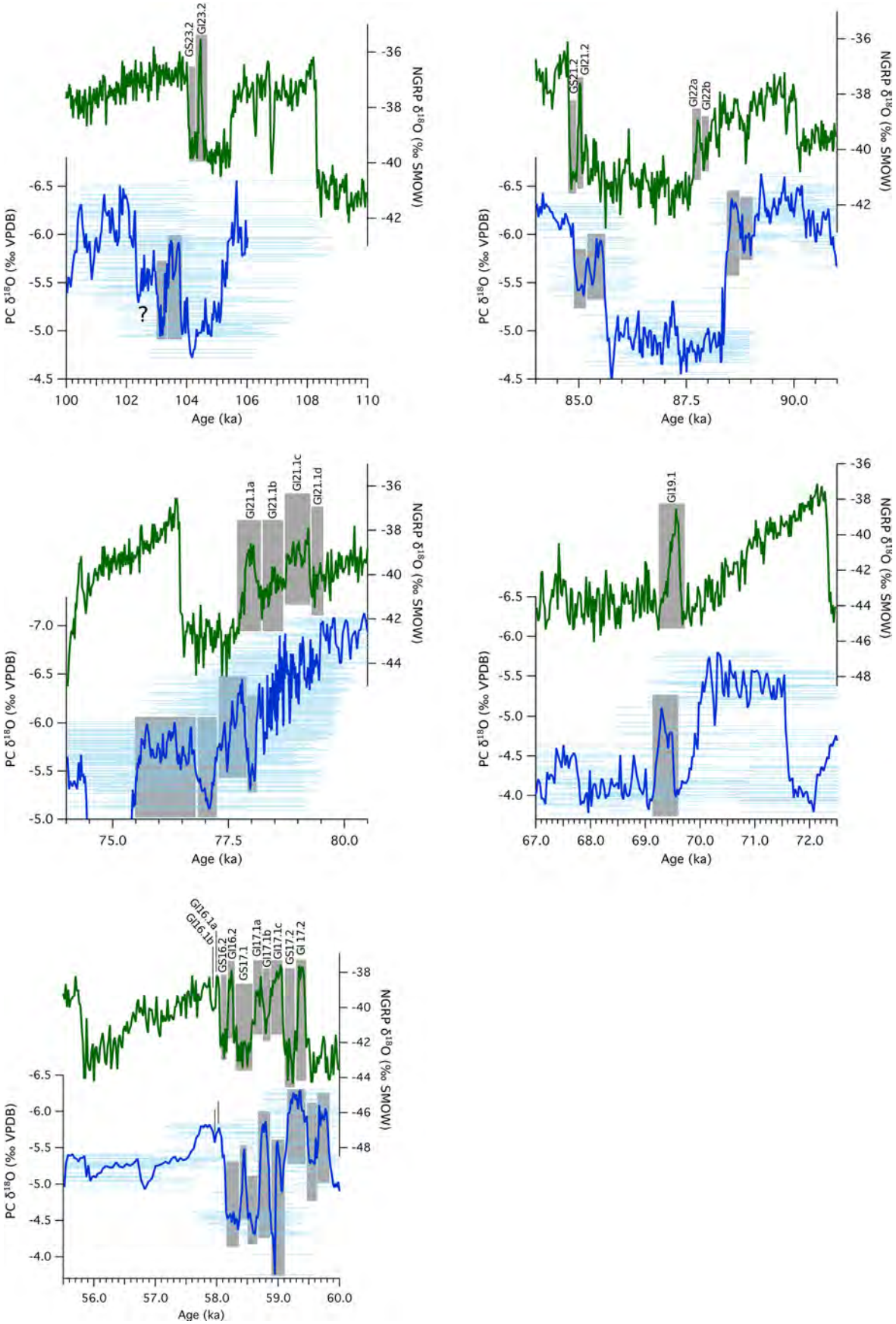

Extended Data Fig. 2 | Intra-millennia events. Intra-stadial and interstadial events recorded by PC $\delta^{18}O$ compared to Greenland ice core $\delta^{18}O$ (24). The events are reported, in both curves, with grey shading.

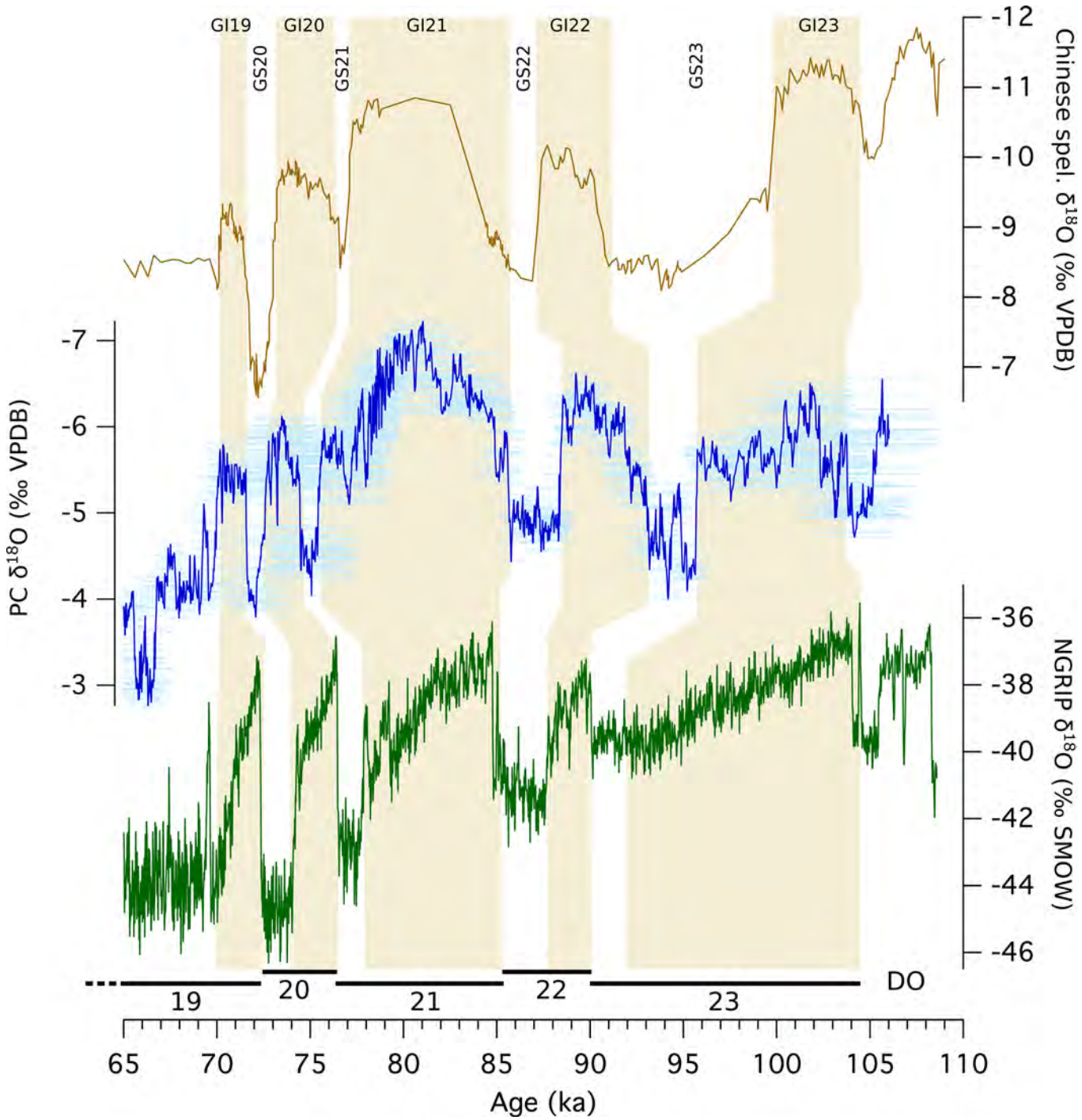

Extended Data Fig. 3 | PC from DO 23 to 19. Similarities between Chinese speleothem $\delta^{18}O$ (orange curve[26]), PC $\delta^{18}O$ (blue curve, this study) and Greenland ice core $\delta^{18}O$ (green curve[15]) from ~110 to ~65 ka, during DO events 23 to 19.

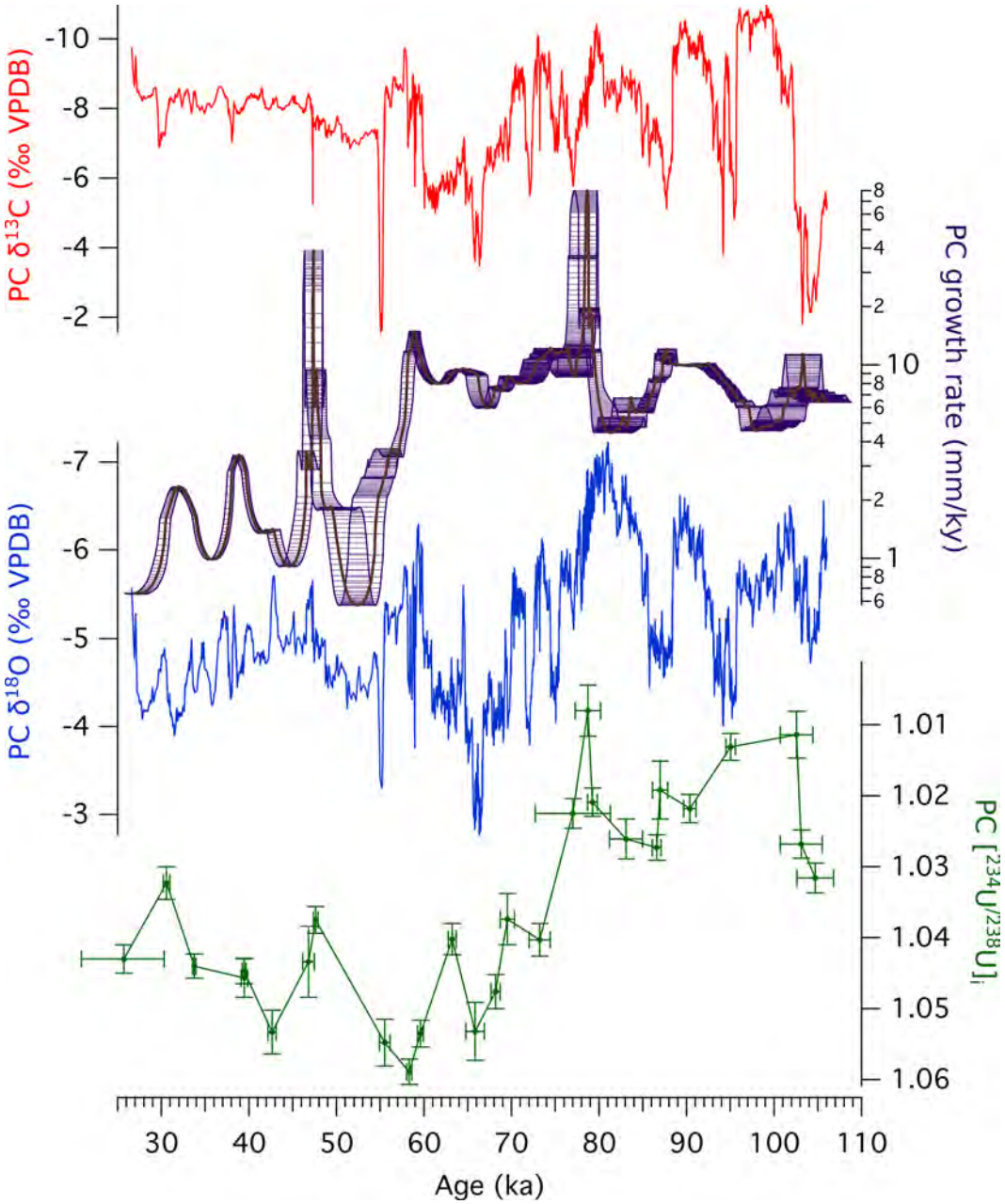

Extended Data Fig. 4 | Growth rate and $[^{234/238}U]_i$. Comparison between PC $\delta^{13}C$, growth rate, $\delta^{18}O$ and $[^{234/238}U]_i$.

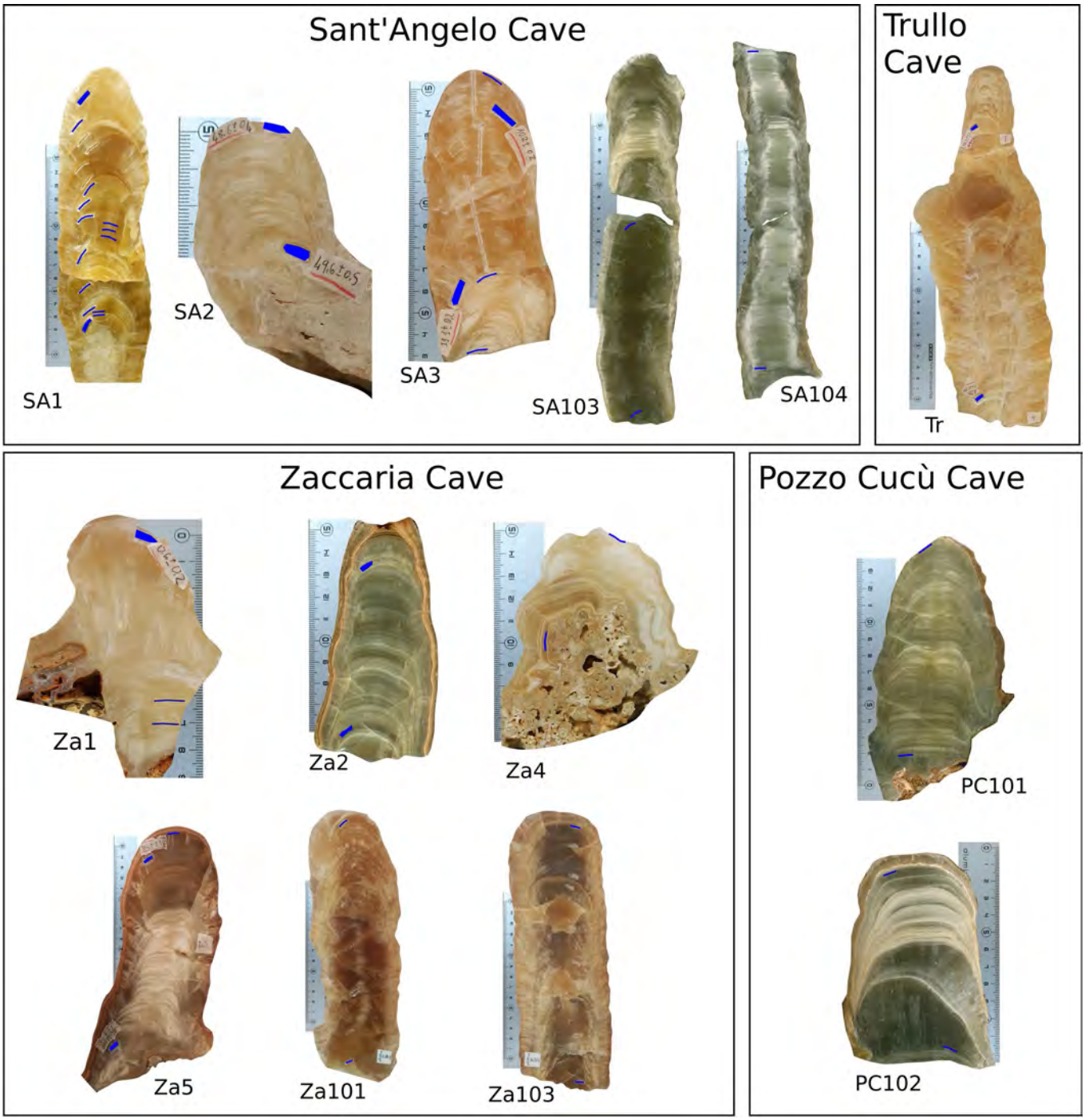

Extended Data Fig. 5 | Materials. Speleothems (except PC, Fig. 1 main text) examined in this study. Blue rectangles indicate the location of sampling for U-Th dating.

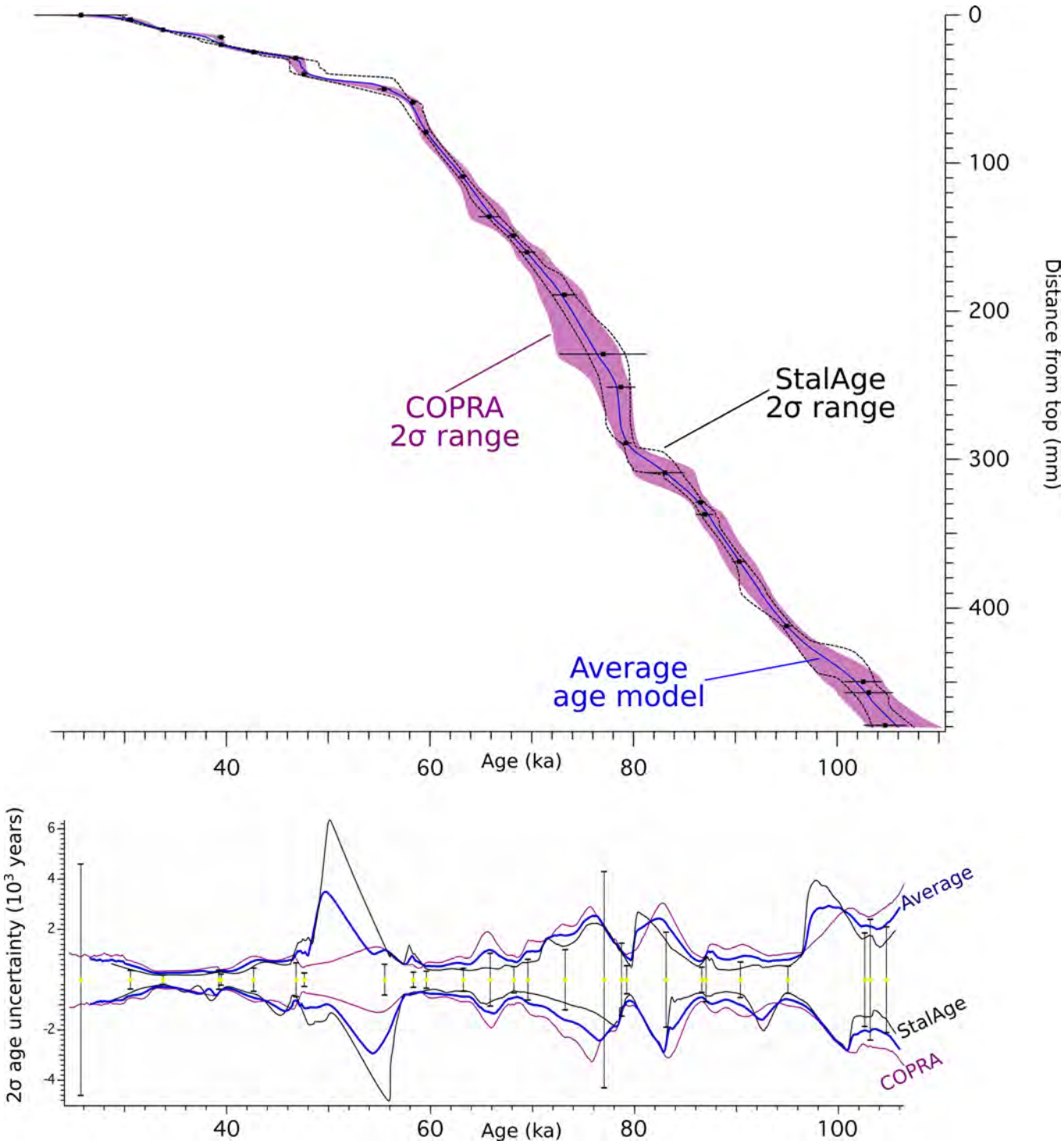

Extended Data Fig. 6 | Age model. Top: comparison between StalAge and COPRA 2σ range and the resulting average age model used in this work. Bottom: Propagation of positive and negative 2σ uncertainty in the various age models. U-Th ages are shown by yellow dots and black 2σ error bars.

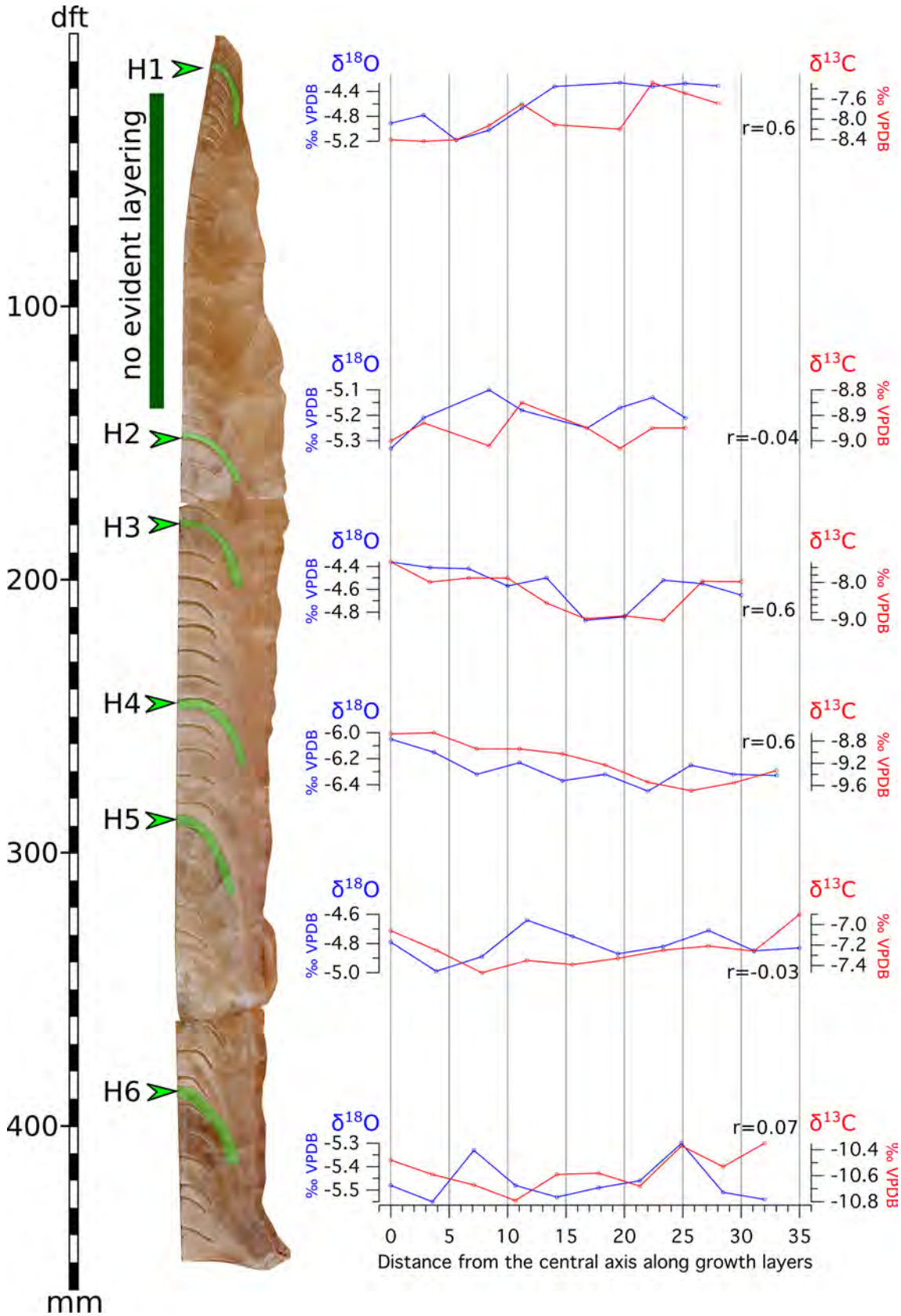

Extended Data Fig. 7 | Hendy test. Subsamples were extracted from individual growth lamina. $\delta^{13}C$-$\delta^{18}O$ correlation (r) provided for each tested layer. The absence of a strong correlation between $\delta^{13}C$ and $\delta^{18}O$ and of a systematic increase from the centre to the flank indicate that calcite was deposited under quasi-equilibrium conditions (see Hendy test discussion for details).